AIP | Journal of Applied Physics

Spin-degenerate surface and the resonant spin lifetime transistor in wurtzite structures

Wan-Tsang Wang, C. L. Wu, J. C. Chiang, Ikai Lo, H. F. Kao, Y. C. Hsu, W. Y. Pang, D. J. Jang, Meng-En Lee, Yia-Chung Chang, and Chun-Nan Chen

Citation: Journal of Applied Physics **108**, 083718 (2010); doi: 10.1063/1.3484042
View online: http://dx.doi.org/10.1063/1.3484042
View Table of Contents: http://scitation.aip.org/content/aip/journal/jap/108/8?ver=pdfcov
Published by the AIP Publishing

Spin-degenerate surface and the resonant spin lifetime transistor in wurtzite structures

Wan-Tsang Wang,[1,a)] C. L. Wu,[1] J. C. Chiang,[1,b)] Ikai Lo,[1] H. F. Kao,[1] Y. C. Hsu,[1] W. Y. Pang,[1] D. J. Jang,[1] Meng-En Lee,[2,c)] Yia-Chung Chang,[3] and Chun-Nan Chen[4]
[1]*Department of Physics, Center for Nanoscience and Nanotechnology, National Sun Yat-Sen University, Kaohsiung 80424, Taiwan*
[2]*Department of Physics, National Kaohsiung Normal University, Yanchao Township, Kaohsiung County 82444, Taiwan*
[3]*Research Center for Applied Sciences, Academia Sinica, Taipei 11529, Taiwan*
[4]*Department of Physics, Tamkang University, Tamsui, Taipei County 25137, Taiwan*

(Received 15 June 2010; accepted 28 July 2010; published online 27 October 2010)

Spin-splitting energies of *wurtzite* AlN and InN are calculated using the linear combination of atomic orbital method, and the data are analyzed utilizing the two-band $\mathbf{k}\cdot\mathbf{p}$ model. It is found that in the $\mathbf{k}\cdot\mathbf{p}$ scheme, a spin-degenerate surface exists in the wurtzite Brillouin zone. Consequently, the D'yakonov-Perel' spin relaxation mechanism can be effectively suppressed for all spin components in the [001]-grown *wurtzite* quantum wells (QWs) at a resonant condition through application of appropriate strain or a suitable gate bias. Therefore, *wurtzite* QWs (e.g., InGaN/AlGaN and GaN/AlGaN) are potential structures for spintronic devices such as the resonant spin lifetime transistor.
 [doi:10.1063/1.3484042]

In recent years a great deal of research in semiconductor physics has been focused on an emerging field—spintronics. Spintronics is a multidisciplinary field whose central theme is the active manipulation of the spin property of electrons. As for implementation of the research efforts on electronic devices, one of the most promising proposals is the spin transistor by Datta and Das.[1] The attractive feature of their spin-field effect transistor (SFET) is that it controls the spin by the gate bias instead of external magnetic field. Recently a similar type of spin transistor, the resonant spin lifetime (RSL) transistor, was proposed.[2–4] The RSL transistor, whose basic idea is very similar to that of the SFET, works in the drift-diffusive regime rather than in the ballistic regime, and therefore lithographical and processing requirement can be lessened. The RSL transistor is designed upon the special properties of the spin lifetime tensor due to the interplay between bulk inversion asymmetry (BIA) and structure inversion asymmetry (SIA) in *zinc-blende* or *wurtzite* quantum wells (QWs). In [hkl]-grown *zinc-blende* QWs, BIA yields not only a cubic-k term but also a linear-k term (called Dresselhaus effect), while SIA yields mainly a linear-k term (called Rashba effect). When the linear-k terms caused by BIA and SIA cancel each other, the electron system reaches the resonant condition based on the D'yakonov-Perel' (DP) spin relaxation mechanism,[5] and the spin direction of electrons can be maintained during the transport process. The spin lifetime resonance occurs only for a single lifetime component in [110]- or [001]-grown *zinc-blende* QWs. However, it takes place for all three spin lifetime components in [111]-grown *zinc-blende* QWs. Such special property in [111]-grown *zinc-blende* QWs can lead to relaxation of design constraints in devices such as the spin-LED or the RSL transistor. In this paper, we shall demonstrate that the spin lifetime resonance also occurs for all three spin lifetime components in [001]-grown *wurtzite* QWs; moreover, the resonance occurs when the spin splitting vanishes to the third order in k, due to the existence of a spin-degenerate surface in the wurtzite Brillouin zone. To demonstrate this, we utilize the spin-orbital component of the *wurtzite* two-band $\mathbf{k}\cdot\mathbf{p}$ Hamiltonian, $H_{SO}(\vec{k})=[\alpha_R-\gamma_{wz}(k_\parallel^2-bk_z^2)](\sigma_x k_y-\sigma_y k_x)$,[6] whose parameters α_R, γ_{wz}, and b are obtained by fitting the spin-splitting energy data from the linear combination of atomic orbital (LCAO) method.

To calculate the spin-splitting energies in AlN and InN, the nearest-neighbor LCAO method is used. The LCAO Hamiltonian $H(\vec{k})$ can be written in the following form:

$$H(\vec{k}) = H_0(\vec{k}) + H_{SO} = \begin{bmatrix} H_0^{\alpha\alpha}(\vec{k}) & 0 \\ 0 & H_0^{\alpha\alpha}(\vec{k}) \end{bmatrix} + \begin{bmatrix} H_{SO}^{\uparrow\uparrow} & H_{SO}^{\uparrow\downarrow} \\ H_{SO}^{\downarrow\uparrow} & H_{SO}^{\downarrow\downarrow} \end{bmatrix}, \quad (1)$$

where $H_0^{\alpha\alpha}(\vec{k})$ is the Hamiltonian without spin-orbit terms ($\alpha=\uparrow$ or $\downarrow$), $\vec{k}=\vec{k}_\parallel+\hat{z}k_z=k_\parallel(\hat{x}\cos\theta+\hat{y}\sin\theta)+\hat{z}k_z$, $\vec{k}_x\|\Gamma\vec{M}$, and $\vec{k}_y\|\Gamma\vec{K}$. The renormalized spin-orbit splittings of the anion-N, cation-Al, and cation-In p states (i.e., $\Delta_N=9$ meV, $\Delta_{Al}=24$ meV, $\Delta_{In}=392$ meV) used in H_{SO} have been reported in Refs. 7 and 8. When crystal field is taken into account, the band structure of the *real* wurtzite is obtained by differentiating the bond in the [001] direction from three other bonds.[9] The corresponding LCAO parameters used in $H_0(\vec{k})$ are obtained through Harrison's d^{-2} rule[10–12] and modification of Slater–Koster coefficients[13] from those in the *ideal* wurtzite.[14] The lattice constants and the internal parameter u of the *real* wurtzite AlN used in $H_0(\vec{k})$ are adopted from Figs. 1(b) and 1(d) of Ref. 15, respectively. The LCAO

[a)]Electronic mail: winstonwwt@gmail.com.
[b)]Electronic mail: chiang@mail.phys.nsysu.edu.tw.
[c)]Electronic mail: melee@nknucc.nknu.edu.tw.

TABLE I. Nearest-neighbor tight binding parameters (in eV) for wurtzite AlN and InN. When crystal field is included, the nearest-neighbor couplings in the bond along the [001] direction (in parentheses) are different from those in three other bonds (see Ref. 14). The values of lattice constants (c,a) and the internal parameter (u) were given in Ref. 15. For the *ideal* wurtzite, $V(s,s)=4E_{ss}$, $V(sa,pc)=\sqrt{3}/4E_{sp}$, $V(pa,sc)=\sqrt{3}/4E_{ps}$, $V(x,y)=4/3(E_{pp\sigma}-E_{pp\pi})$, and $V(x,x)=4/3(E_{pp\sigma}+2E_{pp\pi})$.

Parameter	AlN	InN
E_{sa}	−12.104	−11.900
E_{pa}	3.581	0.500
E_{sc}	−0.096	−2.600
E_{pc}	9.419	8.000
$E_{ss}(E'_{ss})$	−2.694 (−2.730)	−1.685 (−1.619)
$E_{sp}(E'_{sp})$	3.466 (4.001)	1.764 (1.695)
$E_{ps}(E'_{ps})$	4.178 (4.823)	2.789 (2.680)
$E_{pp\sigma}(E'_{pp\sigma})$	5.825 (5.683)	3.077 (2.956)
$E_{pp\pi}(E'_{pp\pi})$	−0.685 (−0.668)	−0.769 (−0.739)

parameters used for wurtzite InN, due to lack of established results, are obtained by directly fitting the first-principle calculation data.[16] The nearest-neighbor LCAO parameters for both wurtzite AlN and InN in this study are listed in Table I. The spin-splitting energy of the lowest conduction band can be obtained after the eigenvalues of the above Hamiltonian are solved.

The spin-orbital component of the two-band $\mathbf{k}\cdot\mathbf{p}$ Hamiltonian for the wurtzite structure from our analytical derivation can be written as

$$H_{SO}(\vec{k}) = [\alpha_R - \gamma_{wz}(k_{\parallel}^2 - bk_z^2)](\sigma_x k_y - \sigma_y k_x), \tag{2}$$

which is consistent with the derivation from the group theories.[17] Here α_R, γ_{wz}, and b are evaluated by fitting the spin-splitting energy and the minimum-spin-splitting (MSS) surface data from LCAO results. The parameters obtained through these processes for AlN and InN are listed in Table II.

Figure 1 shows the calculated results of spin-splitting energy along $\Gamma\vec{M}$ on several k_z-planes from both the LCAO method and the two-band model. As can be seen, the results from the two-band model are highly in agreement with those from the LCAO method. This indicates the spin-splitting energy and the MSS surface in wurtzite structure can be well described by the two-band $\mathbf{k}\cdot\mathbf{p}$ Hamiltonian. Most importantly, in the $\mathbf{k}\cdot\mathbf{p}$ scheme, the spin-degenerate surface does exist in the wurtzite Brillouin zone. Figure 2 shows that the spin-degenerate surface evaluated by two-band $\mathbf{k}\cdot\mathbf{p}$ model is highly in agreement with the MSS surface calculated by the LCAO method. The insets of Fig. 2 schematically depict that the spin-degenerate surface for the real wurtzite AlN (InN) has the shape of a hyperboloid of two sheets (a hyperboloid of one sheet). The two-sheet hyperboloidal spin-degenerate

TABLE II. Parameters for the two-band $\mathbf{k}\cdot\mathbf{p}$ model at zero gate bias.

Parameter	AlN	InN
γ_{wz}(meV Å^3)	−6.445	−353.576
b	3.767	4.885
α_R(meV Å)	0.719	−13.096

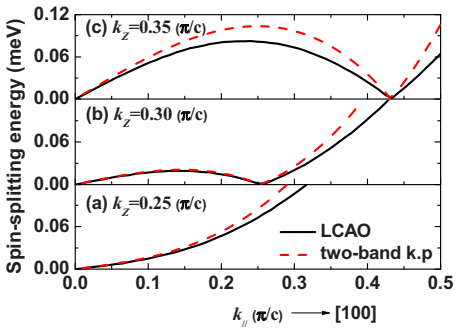

FIG. 1. (Color online) Spin-splitting energy for wurtzite AlN calculated by the LCAO method and fitting by the two-band $\mathbf{k}\cdot\mathbf{p}$ model on different planes (a) $k_z=0.25\pi/c$, (b) $k_z=0.30\pi/c$, and (c) $k_z=0.35\pi/c$.

surface of AlN has been confirmed by our first-principle calculation. As for InN, the characteristics of its spin-degenerate surface are currently under investigation, and will be reported in the near future.

The working principle of the RSL transistor is related to the DP relaxation mechanism. When spin splitting vanishes, the scattering process due to this mechanism is suppressed and the spin lifetime increases dramatically. Consequently, the spin direction of the charge current can be maintained when electrons pass through the channel, and therefore resistance is reduced in the transistor.[3] As a result, it is important to study the relation between the spin-degenerate surface and the spin lifetime. In the two-band $\mathbf{k}\cdot\mathbf{p}$ model, the inversion-asymmetry term of the two-dimensional Hamiltonian for [001]-grown *wurtzite* QWs can be written as $\boldsymbol{H}_{\mathrm{IA}}(\boldsymbol{k})=[\alpha_R - \gamma_{wz}(k_{\parallel}^2 - b\langle k_z^2\rangle)](\sigma_x k_y - \sigma_y k_x)$, and the effective spin-splitting

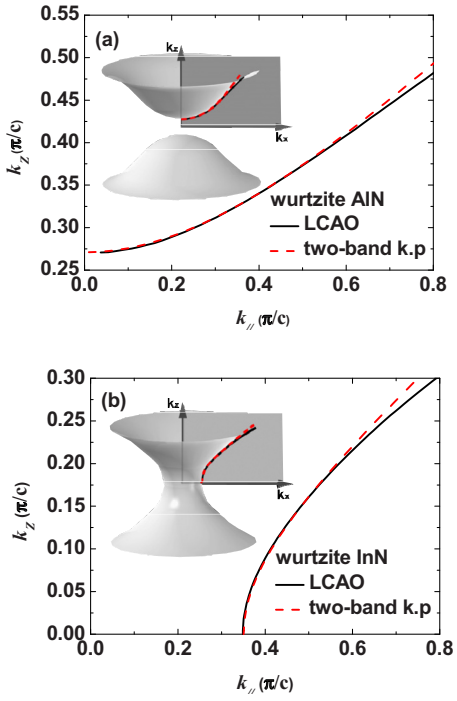

FIG. 2. (Color online) Projections of the MSS surface (solid curve) and the reference spin-degenerate surface (dashed curve) onto the plane of $k_y=0$ for (a) AlN and (b) InN. The equations of the reference spin-degenerate surface for AlN (InN) is $k_{\parallel}^2=3.767\ k_z^2-0.275$ ($k_{\parallel}^2=4.885\ k_z^2+0.121$). The insets depict the projections of the three-dimensional MSS surfaces onto the k_x-k_z plane.

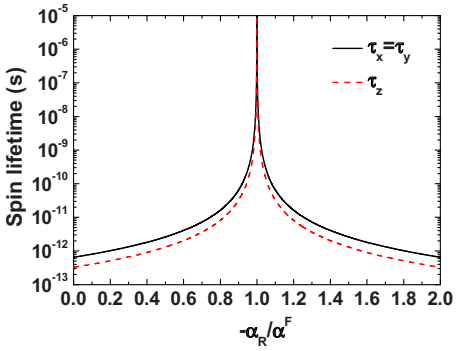

FIG. 3. (Color online) Three components of spin lifetimes for [001]-grown wurtzite InN QWs as the functions of $-\alpha_R/\alpha^F$ ($\alpha^F \equiv \gamma_{wz} b\langle k_z^2\rangle - \gamma_{wz} k_F^2$).

energy becomes $\delta E(k)=2(\alpha_{IA}k_\parallel - \gamma_{wz}k_\parallel^3)$, where $\alpha_{IA}=\alpha_R + \gamma_{wz}b\langle k_z^2\rangle$ and α_R is the coefficient of the Rashba linear-k term. Clearly, a spin-degenerate Fermi surface denoted by $\alpha_R+\gamma_{wz}b\langle k_z^2\rangle - \gamma_{wz}k_F^2=0$ can be achieved in the two-dimensional electron gases (2DEGs) of wurtzite heterostructures, by varying gate voltage, crystal field, or biaxial strain (corresponding to α_R), QW width (corresponding to $b\langle k_z^2\rangle$), or carrier concentration (corresponding to k_F).[17–19] At relatively small carrier concentration, the cubic-k term $[\boldsymbol{H}_{\mathrm{IA},3}(\boldsymbol{k})=-\gamma_{wz}k_\parallel^2(\sigma_x k_y - \sigma_y k_x)]$ in $\boldsymbol{H}_{\mathrm{IA}}(\boldsymbol{k})$ can be neglected, and therefore the inversion-asymmetry term of the two-dimensional Hamiltonian for [001]-grown wurtzite QWs can be approximated by the linear-k term $[\boldsymbol{H}_{\mathrm{IA}}(\boldsymbol{k})\approx \boldsymbol{H}_{\mathrm{IA},1}(\boldsymbol{k}) = \alpha_{IA}(\sigma_x k_y - \sigma_y k_x)]$. Since the linear-$k$ term $\boldsymbol{H}_{\mathrm{IA},1}(\boldsymbol{k})$ of the *wurtzite* [001] structures is identical to that of the *zinc-blende* [111] structures (see Eq. 5 of Ref. 4), the spin relaxation time given in Eq. 6 of Ref. 4 also holds here

$$\tilde{\tau}_x = \tilde{\tau}_y = 2\tilde{\tau}_z = \frac{\hbar^2}{2\tilde{\tau}_1 k_\parallel^2}\frac{1}{\alpha_{IA}^2}, \tag{3}$$

where the tilde indicates a magnitude evaluated at a given energy and $\tilde{\tau}_1$ is the effective time for field reversal due to the harmonic $\ell=1$ of the scattering cross section, and in general $\tilde{\tau}_l^{-1}(E)=\oint\sigma(\phi,E)(1-\cos l\phi)d\phi$.[4] However, when the cubic-k term is also taken into account, the spin lifetimes obtained here will be different from those in Eq. 10 of Ref. 4, due to $\boldsymbol{H}_{\mathrm{IA},3}(\boldsymbol{k})$ in [001] *wurtzite* is different from that in [111] *zinc-blende* (see Eq. 9 in Ref. 4). The spin lifetimes obtained here are

$$\tilde{\tau}_x = \tilde{\tau}_y = 2\tilde{\tau}_z = \frac{\hbar^2}{2\tilde{\tau}_1 k_\parallel^2}\frac{1}{(\alpha_{IA} - \gamma_{wz}k_\parallel^2)^2}. \tag{4}$$

As pointed out in Ref. 4, including the $k_\parallel^6$ term in the denominator of Eq. (4) is not correct in general. However, the $k_\parallel^6$ term is still kept here, since it is correct in the special case when $\alpha_{IA}=0$.

The spin lifetimes $\tau_i=\tilde{\tau}_i(k_F)$ $(i=x,y,z)$ calculated by Eq. (4) for InN are plotted as functions of $-\alpha_R/\alpha^F$ ($\alpha^F \equiv \gamma_{wz}b\langle k_z^2\rangle - \gamma_{wz}k_F^2$) in Fig. 3, with $k_\parallel=k_F=0.01$ Å^{-1}, $\tilde{\tau}_1=1$ ps, $\gamma_{wz}=-353.576$ meV Å^3, $b=4.885$, and $\langle k_z^2\rangle = 0.0439$ Å^{-2}. It is seen that all three spin lifetime components show a resonant behavior when the Fermi surface is spin-degenerate (i.e., $\alpha_R=-\alpha^F$). Such results demonstrate

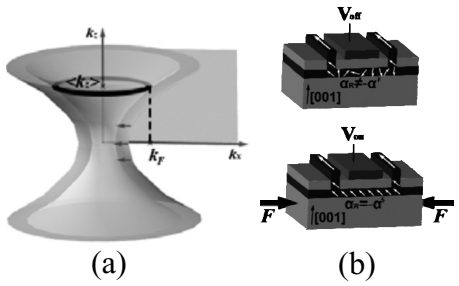

FIG. 4. For [001]-grown wurtzite QWs: (a) by appropriate strain or gate bias, the spin-degenerate surface can be altered and overlapped with the Fermi surface to achieve the resonance. (b) The strain or gate bias drives the lifetime of the injected spins off- or on-resonance. In the off state, the spins are randomized before reaching the collector. In the on state, the spin lifetime increases dramatically and the spin direction can be maintained across the channel of the RSL transistor.

that the DP spin relaxation mechanism can be effectively suppressed for all three spin lifetime components in [001]-grown *wurtzite* QWs at the resonant condition through appropriate device design or application of a suitable gate bias. The spin lifetime $\tilde{\tau}_x(=\tilde{\tau}_y)$ for [111]-grown *zinc-blende* QWs with the cubic-k term $\boldsymbol{H}_{\mathrm{IA},3}(\boldsymbol{k})$ included in the Hamiltonian can be expressed in the following form:[4]

$$\tilde{\tau}_x = \tilde{\tau}_y = \frac{\hbar^2}{2\tilde{\tau}_1 k_\parallel^2}\frac{1}{(\alpha_{IA} - \gamma'_{zb}k_\parallel^2)^2 + \left(\sqrt{\frac{2\tilde{\tau}_3}{\tilde{\tau}_1}}\gamma'_{zb}k_\parallel^2\right)^2}, \tag{5}$$

where $\gamma'_{zb}=\gamma/(2\sqrt{3})$ and γ is the coefficient of the cubic-k term in the BIA Hamiltonian for *zinc-blende* in Ref. 4. Apparently, $\tilde{\tau}_x(=\tilde{\tau}_y)$ of [111]-grown *zinc-blende* QWs always exhibits a finite value as long as $k_\parallel$ and α_{IA} are not equal to zero at the same time. By contrast, the spin lifetime of [001]-grown *wurtzite* QWs diverges when $\alpha_{IA}=\gamma k_\parallel^2$, according to Eq. (4). This difference suggests that, from the perspective of achieving the resonant condition with less constraint, the [001]-grown *wurtzite* QW is a more suitable structure for fabricating the RSL transistor.

Figure 4 depicts that the shape of the spin-degenerate surface can be manipulated via strain or gate bias. For 2DEGs in InN/InAlN QWs, when the compressive strain is applied along the x-y plane, the curvature of the spin-degenerate surface can be altered. If the device is designed appropriately, the strain can be adjusted so that the spin-degenerate surface and the Fermi surface overlap. The gate bias also plays a similar role which is able to modify the shape of the spin-degenerate surface, and leads the electrons to achieve the resonant condition. Likewise, optical illumination may be used to vary the carrier concentration which would consequently change the location of the Fermi surface.

Phenomena related to the spin-degenerate surface indeed have been observed experimentally by Lo *et al.*, since they observed a dramatic change on the spin-splitting energy from 0 to 10 meV at the Fermi surface by varying carrier concentrations in the 2DEGs of GaN/AlGaN wurtzite heterostructures.[18–20] Moreover, the spin-splittmg energies at the Fermi surface of wurtzite III-nitride QWs (e.g., InGaN/AlGaN and InN/AlInN) can also be controlled by gate volt-

age. These observations imply that wurtzite III-nitride QWs, whose spin splitting at the Fermi surface can be degenerate and very sensitive to gate voltage through appropriate sample design, are potential candidates for the RSL transistor.

In conclusion, spin-splitting data of wurtzite AlN and InN calculated by the LCAO method have been analyzed through the two-band $\mathbf{k}\cdot\mathbf{p}$ model. It is found a spin-degenerate surface does exist in the wurtzite Brillouin zone in the $\mathbf{k}\cdot\mathbf{p}$ scheme. As a result, the DP spin relaxation mechanism can be effectively suppressed for all spin lifetime components in [001]-grown wurtzite QWs at resonance, which can be achieved through the application of appropriate strain, gate bias, or optical illumination. Therefore, not only zinc-blende but also *wurtzite* III-nitride (e.g., InGaN/AlGaN and GaN/AlGaN) QWs are promising structures for spintronic devices such as the RSL transistor.

This project was supported by the National Science Council of Taiwan and Academia Sinica.

[1]S. Datta and B. Das, Appl. Phys. Lett. **56**, 665 (1990).
[2]J. Schliemann, J. C. Egues, and D. Loss, Phys. Rev. Lett. **90**, 146801 (2003).
[3]X. Cartoixà, D. Z.-Y. Ting, and Y.-C. Chang, Appl. Phys. Lett. **83**, 1462 (2003).
[4]X. Cartoixà, D. Z.-Y. Ting, and Y.-C. Chang, Phys. Rev. B **71**, 045313 (2005).
[5]N. S. Averkiev, L. E. Golub, and M. Willander, J. Phys.: Condens. Matter **14**, R271 (2002).
[6]W.-T. Wang, C. L. Wu, S. F. Tsay, M. H. Gau, I. Lo, H. F. Kao, D. J. Jang, M.-E. Lee, Y.-C. Chang, C. N. Chen, H. C. Hsueh, and J.-C. Chiang, Appl. Phys. Lett. **91**, 082110 (2007).
[7]D. J. Chadi, Phys. Rev. B **16**, 790 (1977).
[8]J. C. Phillips, *Bonds and Bands in Semiconductors* (Academic, San Diego, CA, 1973), p. 179.
[9]A. Niwa, T. Ohtoshi, and T. Kuroda, Appl. Phys. Lett. **70**, 2159 (1997).
[10]W. A. Harrison, Phys. Rev. B **14**, 702 (1976).
[11]W. A. Harrison and S. T. Pantilides, Phys. Rev. B **14**, 691 (1976).
[12]W. A. Harrison, *Electronic Structure and the Properties of Solids* (Dover, New York, 1989).
[13]J. C. Slater, and G. F. Koster, Phys. Rev. **94**, 1498 (1954)
[14]A. Kobayashi, O. F. Sankey, S. M. Volz, and J. D. Dow, Phys. Rev. B **28**, 935 (1983).
[15]J.-M. Wagner and F. Bechstedt, Phys. Rev. B **66**, 115202 (2002).
[16]J. Furthmüller, P. H. Hahn, F. Fuchs, and F. Bechstedt, Phys. Rev. B **72**, 205106 (2005).
[17]V. I. Litvinov, Appl. Phys. Lett. **89**, 222108 (2006).
[18]I. Lo, M. H. Gau, J. K. Tsai, Y. L. Chen, Z. J. Chang, W. T. Wang, J.-C. Chiang, and T. Aggerstam, Phys. Rev. B **75**, 245307 (2007).
[19]I. Lo, J. K. Tsai, W. J. Yao, P. C. Ho, L. W. Tu, T. C. Chang, S. Elhamri, W. C. Mitchel, K. Y. Hsieh, J. H. Huang, H. L. Huang, and W. C. Tsai, Phys. Rev. B **65**, 161306R (2002).
[20]K. Tsubaki, N. Maeda, T. Saitoh, and N. Kobayashi, Appl. Phys. Lett. **80**, 3126 (2002).